LASER INTERFEROMETER GRAVITATIONAL WAVE OBSERVATORY
- LIGO -
CALIFORNIA INSTITUTE OF TECHNOLOGY
MASSACHUSETTS INSTITUTE OF TECHNOLOGY

Technical Note	**LIGO-T2400203–**	2024/10/16

Final Report LIGO SURF 2024: Quantum Noise Locking on Squeezed States

Jacob Cherry Sam

California Institute of Technology
LIGO Project, MS 18-34
Pasadena, CA 91125
Phone (626) 395-2129
Fax (626) 304-9834
E-mail: info@ligo.caltech.edu

Massachusetts Institute of Technology
LIGO Project, Room NW22-295
Cambridge, MA 02139
Phone (617) 253-4824
Fax (617) 253-7014
E-mail: info@ligo.mit.edu

LIGO Hanford Observatory
Route 10, Mile Marker 2
Richland, WA 99352
Phone (509) 372-8106
Fax (509) 372-8137
E-mail: info@ligo.caltech.edu

LIGO Livingston Observatory
19100 LIGO Lane
Livingston, LA 70754
Phone (225) 686-3100
Fax (225) 686-7189
E-mail: info@ligo.caltech.edu

http://www.ligo.caltech.edu/

Abstract

Gravitational wave detectors are highly sensitive instruments and are affected by a large number of noise sources. Quantum noise, originating from the vacuum field fluctuations that enter the anti-symmetric port of the interferometer, is one of the fundamental sources that affect its sensitivity. Squeezed states are used to tackle this problem as they can have lower fluctuations in a desired quadrature (squeezed quadrature) than the vacuum state. Squeezed states are represented as an ellipse in the quadrature plane. Noises in the interferometer can alter the orientation of this ellipse, which can result in coupling to the anti-squeezed quadrature, degrading the detection. This project aims to characterise a technique called noise locking to lock the squeeze angle and thus maintain the orientation of the ellipse. This technique can be used for vacuum-squeezed states and does not involve another phase reference other than the squeeze angle, which makes it experimentally simpler. This technique is modelled in an electronically simulated system of squeezing to investigate its performance. The future aim is to acquire and impart this technique onto the squeezed state in a Waveguide Optical Parametric Amplification (WOPA) system.

Contents

1 Introduction

1.1 Gravitational Waves and LIGO

The Laser Interferometer Gravitational-Wave Observatory (LIGO) uses large-scale specialised Michelson Interferometers, operating on a dark fringe with 4km arms, to detect the quadrupole signals of Gravitational Waves from astronomical sources. The LIGO observatories are located at Hanford, Washington and Livingston, Louisiana, in the USA, along with the upcoming joint India-US detector - LIGO India. Fabry-Perot cavities are used in the arms of the detector to increase the time of interaction with gravitational waves, along with employing power recycling and signal recycling to enhance the laser power and frequency response, respectively. Considerable improvement was attained while moving to the Advanced LIGO (aLIGO) from the initial LIGO, which includes an improvement by a factor of 10 in the strain sensitivity in the region around 100 Hz, and the low-frequency end of the bandwidth was moved to 10 Hz from 40 Hz [1]. The detection of gravitational waves is affected by a number of different noise sources, and thus, the aim of every upgrade of the detector is to suppress the noise level arising from these various sources. The noise level affecting the detection sensitivity of LIGO is shown below:

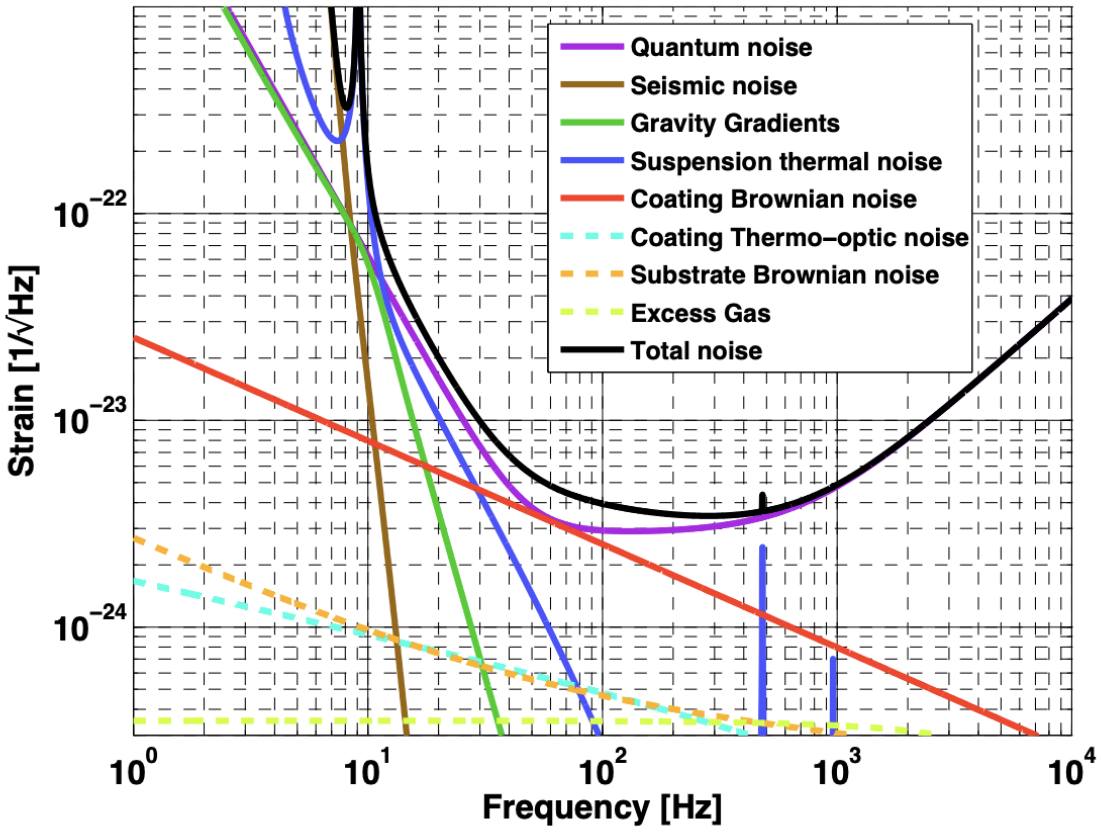

Figure 1: Noise Budget of LIGO [2]

1.2 Quantum Noise

Quantum Noise affects the detection of Gravitational Wave Detectors in a large region of its detection bandwidth and imposes a fundamental limit on the sensitivity of measurement, making mitigating quantum noise an essential task. Quantum Noise, which includes Shot Noise (fluctuations in photon number on the photodetector which results in fluctuating power measurement) and Radiation Pressure Noise (fluctuations of photons reflecting from the suspended test masses causing them to move), originates from the vacuum field that enters the anti-symmetric port of the interferometer [3].

As a consequence of Heisenberg's uncertainty principle with the non-commuting property of position and momentum observables, the two quantum noises described above set the Standard Quantum Limit (SQL) as the optimal sensitivity obtainable without using any Quantum Non-Demolition techniques. The strain sensitivity SQL of a Michelson Interferometer is given as:

$$h_{SQL} = \sqrt{\frac{4\hbar}{m\Omega^2 L^2}}$$

where Ω is the angular measurement frequency, m is the mass of the test mass, and L is the arm length of the interferometer [4].

1.3 Squeezed States

Squeezed states of light are states in which the noise of the electric field is below that of the vacuum state at certain phases [5]. Using these non-classical states of light allows us to breach the SQL, thus improving the detectors' sensitivity.

The Amplitude quadrature, X_1 and the Phase quadrature, X_2, can be expressed in terms of the bosonic creation and annihilation operators as expressed in the following:

$$a = \frac{(X_1 + iX_2)}{2}$$

$$a^\dagger = \frac{(X_1 - iX_2)}{2}$$

The non-commuting nature of the Amplitude and Phase quadratures results in the following uncertainty relation:

$$\Delta X_1 \Delta X_2 \geq 1$$

where ΔX represents the standard deviation of the observable X.

The coherent state and vacuum state are minimum uncertainty states with $\Delta X_1 = 1$ and $\Delta X_2 = 1$, with the difference being that vacuum states have zero coherent amplitude, and the coherent states have non-zero coherent amplitude. Squeezed states, on the other hand,

have the standard deviation of one of the quadratures below 1 and, as a result, will have the standard deviation of the orthogonal quadrature to be above 1, satisfying the uncertainty relation. These states can be expressed as Wigner functions in the following figure.

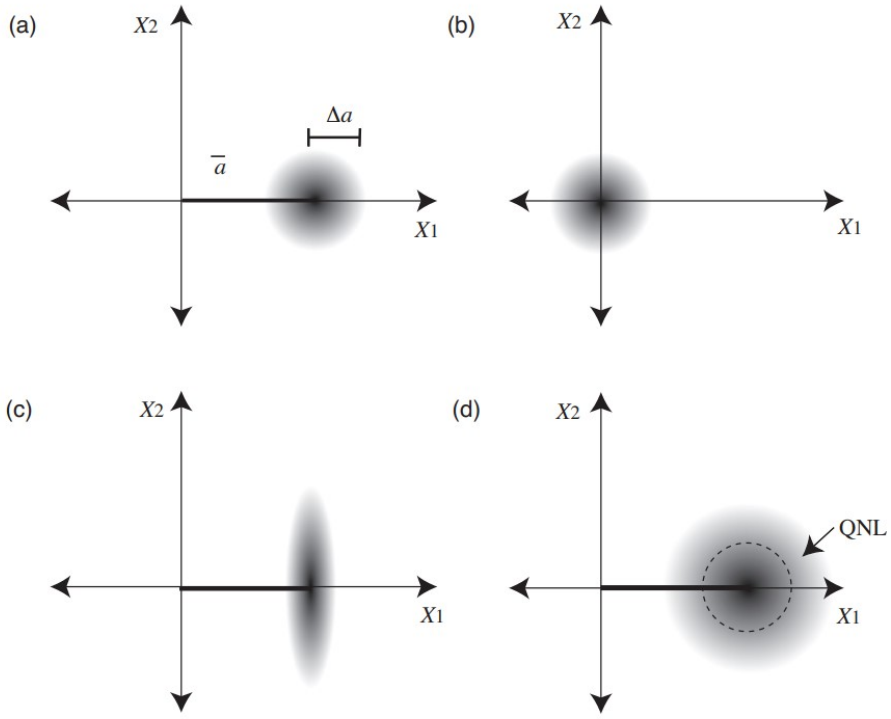

Figure 2: Wigner functions for a) The coherent state, b) The vacuum state, c) The Amplitude Squeezed state d) The Noisy state [4]

From the figure, it can be seen that the process of squeezing improves the noise in one quadrature, but at the same time, the noise in the other quadrature increases in order to satisfy the uncertainty relation. Hence, squeezing is a clever way to manipulate the uncertainties in such a way that the fluctuations in one quadrature go below the quantum limit at the expense of increased fluctuation at the orthogonal quadrature. So, if the measurement is made along the squeezed quadrature, we have lesser noise and if the measurement is made along the anti-squeezed quadrature, we have larger noise than the shot noise level.

1.4 Schemes of squeezing

Squeezing is primarily produced using the non-linear effects of crystals. These processes can generate a beam with a frequency distinct from that of the input beam. The following image is the schematic of the Optical Parametric Oscillator (OPO), which is the scheme used for generating squeezing in LIGO.

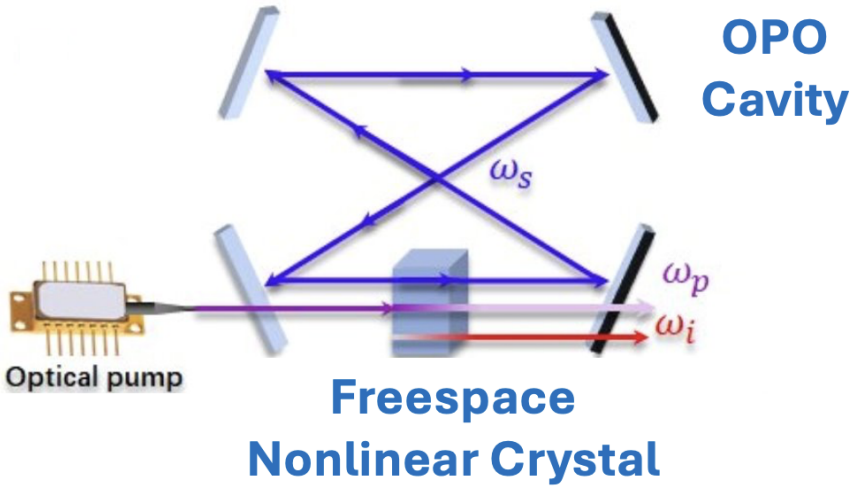

Figure 3: Schematic of Optical Parametric Oscillator

This uses a bow-tie type cavity to increase the electric field strength in order to produce squeezing using the non-linear crystal. It involves the locking of several cavities, which makes it experimentally difficult and cumbersome. This is the motivation for looking into different schemes for obtaining squeezing.

WOPA (Waveguide Optical Parametric Amplification) is a proposed alternative scheme to produce squeezing. It is a simple pass device which works as shown in the following toy diagram.

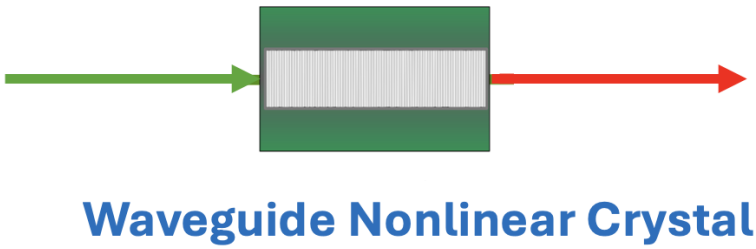

Figure 4: Waveguide Optical Parametric Oscillator

For its working, it does not call for locking of any cavities, which makes it experimentally much more elegant than OPO. Its compact and portable design could facilitate the application of quantum squeezing in other fields. This compactness also presents a significant advantage for the upcoming space interferometer, LISA. On the other hand, the waveguide is micrometres thick, which makes it difficult to match a beam into and out of the waveguide. This can lead to increased matching losses, which can adversely affect the conversion efficiency. Once these challenges are met, WOPA is a compact and simpler alternative to OPO as the squeezer for LIGO.

2 Objective

2.1 Homodyne Phase Locking: A critical requirement

Squeezing is detected through quadrature measurements made with the help of the Balanced Homodyne Detection Technique (discussed later in this report), where a Local Oscillator (LO) is interfered with the squeezed vacuum. This can be visualised in the phase space picture using the following diagram:

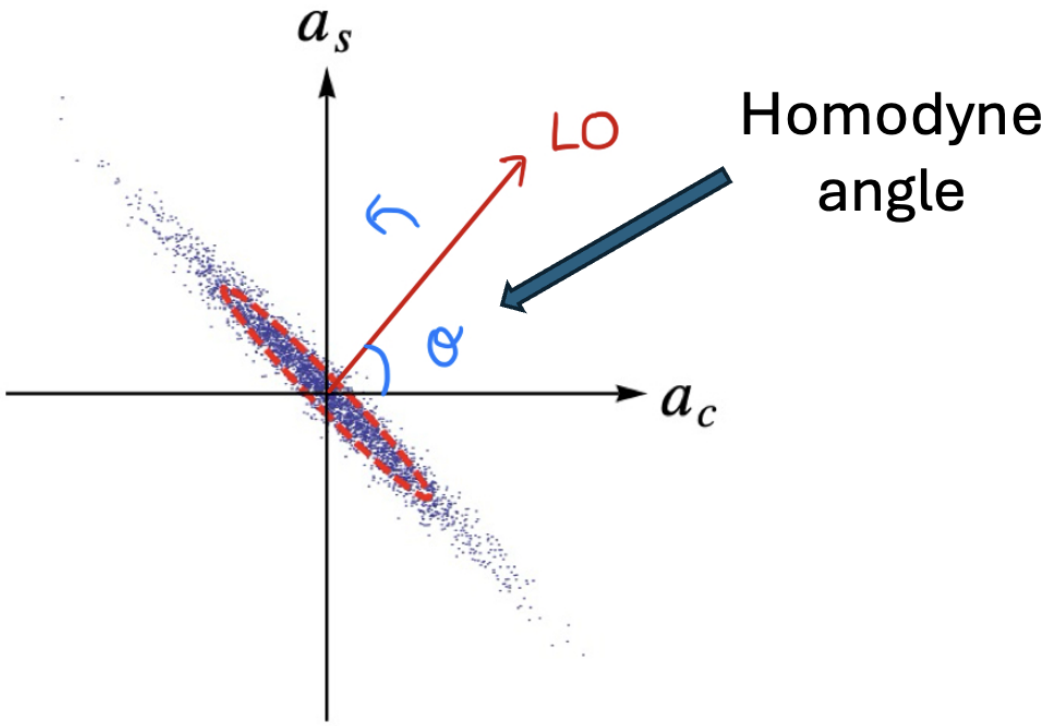

Figure 5: Squeezed vacuum and Local Oscillator

When the LO is along the semi-minor axis of the squeezed vacuum ellipse, we have minimum noise. On the other hand, when it is along the semi-major axis, the noise is maximum and is even higher than the shot noise level present without squeezing. So, in order to breach the quantum limit, it is mandatory to stay at that particular homodyne phase, which corresponds to the minimum noise level.

Squeezing can be achieved at any arbitrary homodyne angle(it can be defined as the angle made by the semi-minor axis of the squeezed ellipse with any one of the quadratures). Interferometric and seismic noises can alter the squeezing angle, resulting in the coupling to the anti-squeezed quadrature, which will adversely affect the sensitivity. Hence, locking the squeezing angle is essential for maintaining the orientation of the squeezed ellipse in the phase space and maintaining the desired level of squeezing. Hence, it is very crucial to lock the homodyne phase so as to stay at the minimum noise level.

2.2 Quantum Noise Locking for Homodyne phase locking

The major aim of the project will be to understand, implement and characterise an elegant homodyne phase locking technique, known as the Quantum Noise Locking (QNL) technique, to control the squeeze angle as described in [6]. This homodyne phase locking technique has to be implemented in the WOPA setup. The optical implementation of WOPA is still in progress, and the primary goal of this project was to characterize the technique of noise locking prior to having the actual optical squeezing setup. For that matter, an electronic simulation of squeezing was attained, and quantum noise locking was employed electronically onto this simulated squeezing to characterise its performance. Once the noise locking was achieved, we obtained the measure of how good the technique was. To acquire this measure, error analysis and stability analysis were performed on the noise locking technique with which the amount of noise that this technique can tolerate was determined.

The subsequent objective would be to achieve squeezing in a waveguide using Waveguide Optical Parametric Amplification (WOPA) and observe the squeezing arcs in the MHz range. The technique of Balanced Homodyne Detection is to be employed to detect the squeezed quadrature. Once squeezing is achieved, the studied technique of quantum noise locking is to be performed to determine the performance of the lock on optical squeezers.

Once quantum noise locking is achieved and well understood, a promising objective is to obtain the locking in the audio frequency range (up to a few kHz) by performing the necessary circuit noise analysis and setting up readout optics and electronics pertaining to lower frequencies. The successful outcome would be obtaining the stable locking of the squeezing angle in a waveguide having the change of the squeeze angle (phase fluctuation) less than 1 milliradian, which is the level of locking required for Advanced LIGO (aLIGO).

3 Approach and Methodology

3.1 Generating Squeezing

Squeezing is generated by making use of non-linear interactions in crystals. The polarization of a non-linear medium on the application of an Electric field can be expressed as :

$$P = \epsilon_0(\chi_1 E + \chi_2 E^2 + \chi_3 E^3 + ...)$$

where P is the induced Polarisation in the media, E is the Electric field applied, ϵ_0 is the permittivity of free space, and χ_i is the susceptibility of i^{th} order. The χ_2 non-linear media in Periodically Poled Potassium titanyl phosphate (PPKTP) crystal is used to generate squeezing. The χ_2 non-linearity can cause three-wave mixing effects, including Second Harmonic Generation (SHG) and Spontaneous Down Conversion (SPDC) [4]. χ_2 non-linear interactions can be generally classified into up-converting and down-converting processes. Two photons of lower energy are converted into a high-energy photon in the up-converting process, and the complementary of this process, where a photon of higher energy is converted into two lower energy photons, is called a down-converting process.

$$\omega_1 + \omega_2 = \omega_3 \quad \text{up-conversion}$$

$$\omega_3 = \omega_1 + \omega_2 \quad \text{down-conversion}$$

If $\omega_1 = \omega_2$ in the up-converting process, the resulting process is SHG, and in the case of the down-converting process, the resulting process satisfying this property is called degenerate SPDC. In the degenerate SPDC process, the photons generated with lower frequencies are indistinguishable in terms of their frequency, polarisation, and direction. The equations given above impose the conditions for the conservation of energy. It should also be noted that the phase matching conditions are also to be satisfied, which is described below:

$$\vec{k_1} + \vec{k_2} = \vec{k_3}$$

where $\vec{k_i}$ is the wave vector defined by $k_i = \frac{\omega_i n(\omega_i)}{c}$.

This process of SPDC results in a conversion of one photon of higher frequency into two photons of lower energy that are correlated, which results in a squeezed state, which can then be detected by the process of Balanced Homodyne Detection.

3.2 Balanced Homodyne Detection

Balanced Homodyne Detection (BHD) is considered to be the method of choice for performing quadrature measurements. The schematic of the method is shown below:

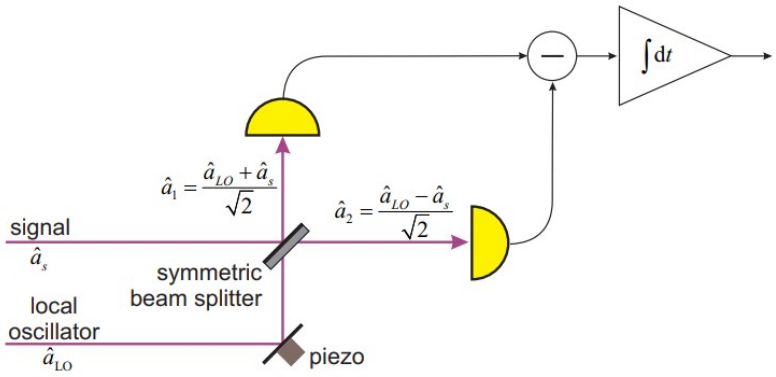

Figure 6: Balanced Homodyne Detection (BHD) [5]

In this technique, the signal field is overlapped on a symmetric beam splitter with a strong laser field known as the Local Oscillator, where the phase of the Local Oscillator is controlled via a piezoelectric transducer. The outputs from the beam splitter reach two photodiodes, and the corresponding photocurrents are subtracted electronically. From this subtracted photocurrent, the quadrature measurement is done by analysing either the time domain or the frequency domain approaches as explained in [5]. The noises that can affect the BHD readout should also be considered.

3.3 Overview of Quantum Noise Locking

The essentiality of this technique to lock the squeeze angle arises for optical states with zero coherent amplitude, such as the squeezed vacuum state for which the usual phase stabilising techniques, including RF modulation/demodulation and DC readout techniques, cannot be used [6]. This technique relies on the asymmetry in the noise of the squeezed and anti-squeezed quadratures. A schematic representation this technique is shown below:

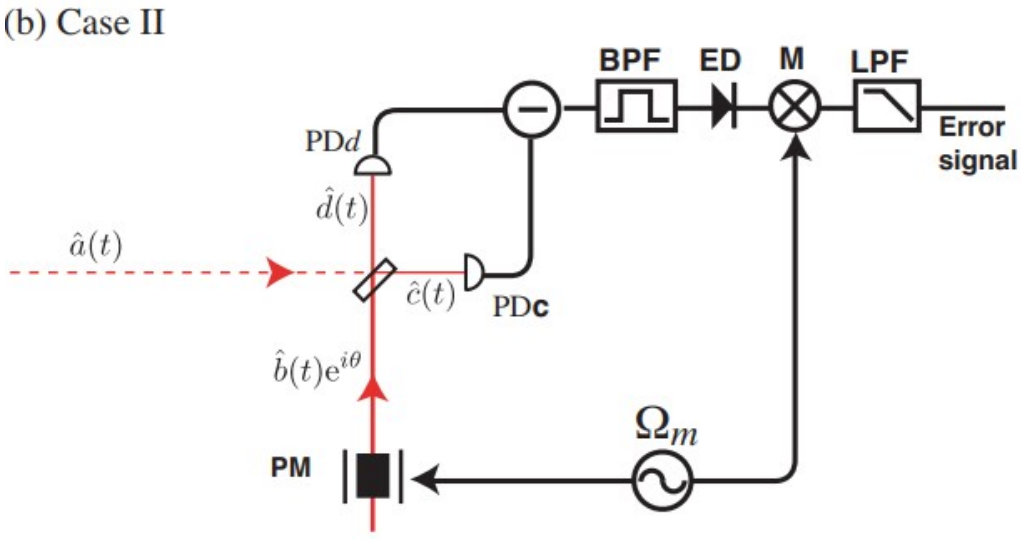

Figure 7: Schematic of Quantum Noise Locking [4]

As seen in the figure, the squeezed state (represented by $\hat{a}$) is interfered with another laser, which is called the local oscillator (represented by $\hat{b}$. There is a relative phase(θ) between these two signals, which is taken into account by the exponential phase factor. The interfered outputs are subtracted electronically in the process of Balanced Homodyne Detection, and the resulting output is as shown below:

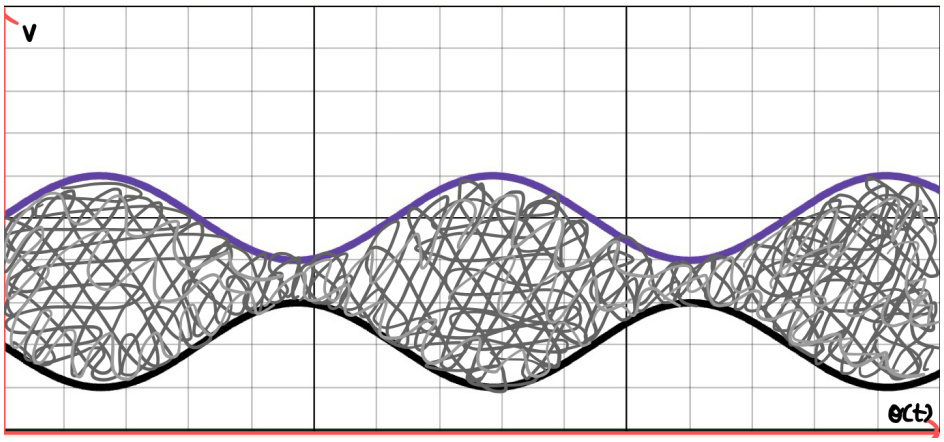

Figure 8: Output of Balanced Homodyne Detection

It is to be noted that the variation in noise level as can be seen in the figure above, is due to squeezing. As a result, at some particular phases, there is maximum noise, and at some other phases, there is minimum noise, and the primary goal of homodyne phase locking is to stay at those particular phases where there is minimum noise.

This output is passed onto a **Bandpass filter**. This is done so as to constrain our frequency to that particular frequency regime where shot noise dominates. The bandpass-filtered output is passed through an envelope detector to read off the noise variation by tracing the envelope of the bandpass-filtered output. Once this is obtained, we need a mechanism to produce a signal for feedback, which dictates the system to lock at that homodyne phase where the noise is minimal. For this, phase modulation is applied to the local oscillator, and thus, the operating point is dithered at every point of the noise amplitude in the envelope detected output. Then, the envelope detected the output is demodulated which results in a signal that detects the slope at every point. This resulting signal is the error signal which has zero crossings at those phases where there is maximum and minimum of the noise amplitude. This error signal is further used for control. The following diagram shows the envelope detected output and the error signal:

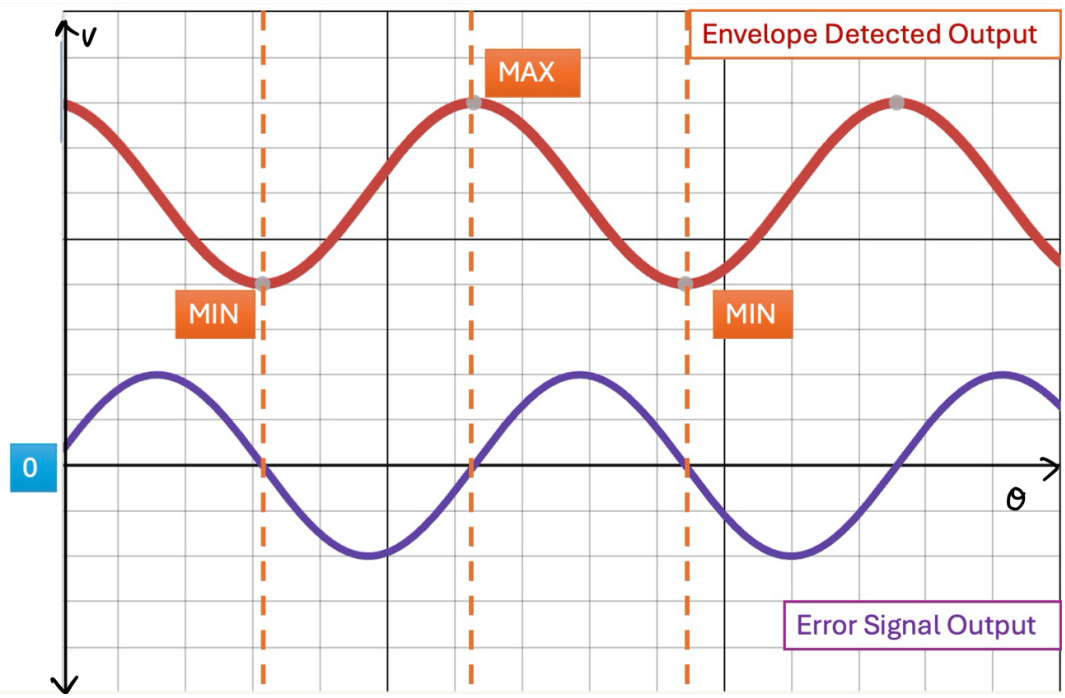

Figure 9: Noise Amplitude and Error Signal

From the figure, it could be seen that the extrema of the noise amplitude corresponds to the phase for which the error signal has zero crossings. This validates the use of this error signal for control, which was obtained by using the noise variation itself as the reference.

4 Modeling

4.1 Mathematical derivation of the error signal

To obtain the error signal, the output of the balanced homodyne detector is bandpass filtered, then envelope detected, which reads out the noise amplitude. The output from the envelope detector is then demodulated and low-pass filtered, and this would produce the required error signal.

The following is the derivation for obtaining the error signal [4].

In the figure above (Figure 7), $\hat{a}(t)$ represents the squeezed state, and $\hat{b}(t)$ represents the Local Oscillator, and each of them can be split into an average component represented by $\bar{s}$ and the time-dependent fluctuating component is represented as $\delta s(t)$. The photocurrents detected in the two photodetectors are electronically subtracted in the process of balanced homodyne detection, and the resulting difference can be split into an average component (no time dependence) and a time-dependent fluctuating component. The fluctuating component is given as follows:

$$\delta i_\theta^-(t) = h\nu \left(\bar{a}\delta X_1^{(b)} \sin\theta + \bar{a}\delta X_2^{(b)} \cos\theta + \bar{b}\delta X_1^{(a)} \sin\theta - \bar{b}\delta X_2^{(a)} \cos\theta \right) \tag{1}$$

From this, the variance of the difference photocurrent can be calculated:

$$V(i_\theta^-) = < |\delta i_\theta^-|^2 > = h^2\nu^2 \left(\bar{a}^2(V_1^{(b)} \sin^2\theta + V_2^{(b)} \cos^2\theta) + \bar{b}^2(V_1^{(a)} \sin^2\theta is + V_2^{(a)} \cos^2\theta) \right) \tag{2}$$

The Local Oscillator is much stronger than the squeezed state, which implies $\bar{a} \ll \bar{b}$, and thus the variance becomes:

$$V(i_\theta^-) = h^2\nu^2\bar{b}^2(V_1^{(a)} \sin^2\theta + V_2^{(a)} \cos^2\theta)$$

$$V(i_\theta^-) = h\nu\bar{P}_{LO}V_\theta$$

where $\bar{P}_{LO} = h\nu\bar{b}^2$ is the power of the local oscillator and V_θ is the variance relative to the shot noise limit which can be written as:

$$V_\theta = V_1^{(a)} \sin^2\theta + V_2^{(a)} \cos^2\theta$$

$$V_\theta = (\frac{V_1^{(a)} + V_2^{(a)}}{2})(1 + \gamma \cos 2\theta(t))$$

where, $\gamma = \frac{|V_2^{(a)} - V_1^{(a)}|}{V_1^{(a)} + V_2^{(a)}}$ and $\theta(t) = \theta_0 + \beta \sin\Omega_m t$, which is because of the relative phase modulation of the input fields with θ_0 being the average phase, β being the modulation depth and Ω_m being the frequency in which the squeeze angle is dithered.

Expanding this in terms of the Bessel functions and neglecting the higher order terms results in:

$$V_\theta \simeq \frac{1}{2}(V_1^{(a)} + V_2^{(a)})\,(1 + \gamma J_0(2\beta)\cos 2\theta_0 - 2\gamma J_1(2\beta)\sin 2\theta_0 \sin\Omega_m t)$$

Thus, the variance of the difference photocurrent would become:

$$V(i_\theta^-) = h\nu\bar{P}_{LO}\frac{1}{2}(V_1^{(a)} + V_2^{(a)})\,(1 + \gamma J_0(2\beta)\cos 2\theta_0 - 2\gamma J_1(2\beta)\sin 2\theta_0 \sin\Omega_m t)$$

The quantum noise locking error signal is obtained from envelope detection followed by demodulation. The demodulation is mathematically described by the multiplication by a sinusoid at the modulation frequency. Thus the error signal is:

$$\xi = V(i_\theta^-) \times \sin(\Omega_m t + \phi_D),$$

After discarding the terms at frequency Ω_m or higher and choosing the demodulation frequency ϕ_D to be 0, the following can be obtained:

$$\begin{aligned}\xi &= -\frac{1}{2}h\nu P_{\rm LO}(V_1^{(a)} + V_2^{(a)})\gamma J_1(2\beta)\sin 2\theta_0 \\ &= -\frac{1}{2}h\nu P_{\rm LO}(V_2^{(a)} - V_1^{(a)})J_1(2\beta)\sin 2\theta_0\end{aligned}$$

which is the required expression for the error signal for the quantum noise locking, which has zero crossing at $\theta_0 = 0$ and $\theta_0 = \pi/2$.

4.2 Noise performance of Noise locking

As seen in the previous section, the error signal is derived using the noise power of the squeezed state itself. Thus, the noise performance would depend on the variance of the variance (noise of the noise of the squeezed state) [4]. This is obtained by taking the kurtosis (fourth order moment of the distribution), which is labelled as ΔV_a^θ. For the amplitude quadrature of the field a, the kurtosis is given by:

$$\Delta V_1^{(a)} = \sqrt{2}V_1^{(a)}$$

Similarly, for the phase quadrature:

$$\Delta V_2^{(a)} = \sqrt{2}V_2^{(a)}$$

It is also possible to obtain the phase fluctuations, $\Delta\theta$, at the two lock points ($\theta_0 = 0, \pi/2$) in terms of the squeezing factor R, the detection loss L and the detection bandwidth $\Delta\Omega$ following the mathematical derivation in [4], and the result is as follows:

$$\Delta\theta|_{\theta_0=\frac{\pi}{2}} \approx \sqrt{\frac{1+\frac{Le^{2R}}{1-L}}{e^{4R}-1}} \left(\frac{2}{\Delta\Omega}\right)^{\frac{1}{4}}$$

$$\Delta\theta|_{\theta_0=0} \approx \sqrt{\frac{1+\frac{Le^{-2R}}{1-L}}{1-e^{-4R}}} \left(\frac{2}{\Delta\Omega}\right)^{\frac{1}{4}}$$

This shows that the stability of the quadrature improves as the squeezing factor is increased. It is also to be noted that the noise performance of the lock improves as the detection bandwidth increases, even though the dependence is weak ($\Delta\Omega^{1/4}$)

4.3 Expected Level of Shot Noise

The level of shot noise can be estimated using the following formula:

$$S_N = \sqrt{2h\bar{P}\nu}$$

where, h is the Planck's constant, $\bar{P}$ is the Power of the Local oscillator and ν is the frequency of the laser used. For this experiment, the power of the light following onto the photodetector (1811 FS) from the balanced homodyne setup was measured to be **0.46 mW**. The wavelength of the laser light used was **1064 nm**.

From these values, S_N was calculated to be $\mathbf{1.3 \times 10^{-11}}$ **W**/$\sqrt{\textbf{Hz}}$. Then, the responsivity of the photodetector was taken into account (**0.70 A/W**) along with the resistance of the Transimpedence Amplifier **40 kΩ** to get the readout in **V**/$\sqrt{\textbf{Hz}}$. From these calculations, the resulting estimated shot noise level was found to be **0.37 uV**/$\sqrt{\textbf{Hz}}$.

On calculating the level of shot noise, it is possible to calculate the level of the squeezed state and the anti-squeezed state for a given level of squeezing. The level of squeezing is represented in decibels using the following formula:

$$\text{Level of Squeezing in dB} = 20 \cdot \log_{10}\left(\frac{V_{\text{SQZ}}}{V_{\text{SHOT}}}\right)$$

$$\text{Anti-Squeezing in dB } 20 \cdot \log_{10}\left(\frac{V_{\text{ANTISQZ}}}{V_{\text{SHOT}}}\right)$$

where V_{SHOT} is the estimated shot noise calculated before, V_{SQZ} and $V_{ANTISQZ}$ are the noises of the squeezed and anti-squeezed quadrature, respectively, that are to be calculated.

For instance, if we are expecting **4dB** squeezing, with the previously calculated level of the shot noise (**0.37 uV**/$\sqrt{\textbf{Hz}}$), the expected noise level of the squeezed and anti-squeezed states would be **0.23 uV**/$\sqrt{\textbf{Hz}}$ and **0.58 uV**/$\sqrt{\textbf{Hz}}$ respectively.

Using these equations, the error signal can be written as a function of the level of squeezing and anti-squeezing in decibels as follows:

$$\xi = -\frac{1}{2} h\nu P_{\mathrm{LO}} \mathrm{V}_{\mathrm{SHOT}} (e^{\frac{y}{20}} - e^{\frac{|x|}{20}}) J_1(2\beta) \sin 2\theta_0$$

where y is the level of anti-squeezing and x is the level of squeezing in dB.

4.4 Obtaining the Error Signal

The final setup, including the generation of squeezed states followed by the setup performing noise locking, is as shown below:

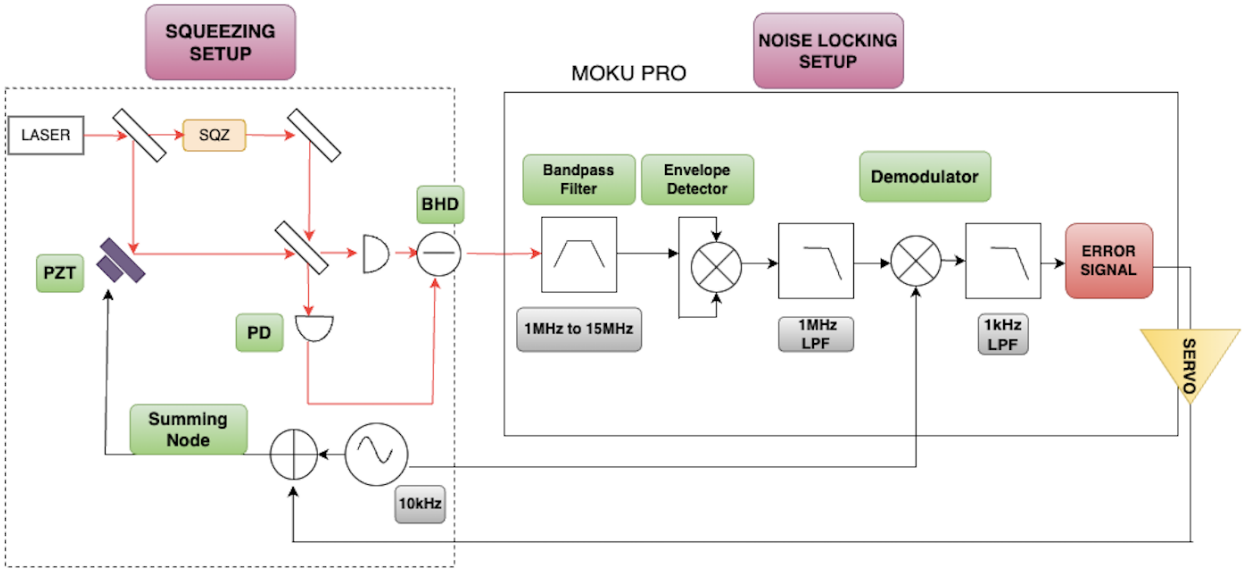

Figure 10: Schematic of the final setup. PZT: Piezoelectric Transducer, PD: Photodetector, BHD: Balanced Homodyne Detector, SQZ: Squeezed state generator, LPF: Low Pass Filter

The initial objective was to characterise the technique of noise locking even before squeezed states were optically generated. For that, the squeezing setup, as depicted in the above figure, was electronically modelled. Further, the noise locking technique was applied to this electronically simulated squeezing output to characterise the performance of the technique.

An electronic setup was modelled that simulated squeezing, and then the quantum noise locking was electronically employed to obtain the error signal. For this, Moku Instruments (MOKU PRO and MOKU Lab), which is composed of a versatile set of high-performing measurement devices, were used. The schematic for obtaining the error signal is shown below:

The DS345 function generator was used to produce a 100 Hz signal with 1 V peak-to-peak amplitude. This corresponds to the disturbance that can cause the squeezing angle to change. A 10 kHz sinusoidal signal is used to phase modulate the 100 Hz signal. This corresponds to the dithering caused by the PZT in the actual optical setup.

The function generator of the Moku Pro is used to generate 1 V peak-to-peak Gaussian noise that corresponds to shot noise. This noise is amplitude-modulated by the signal coming from

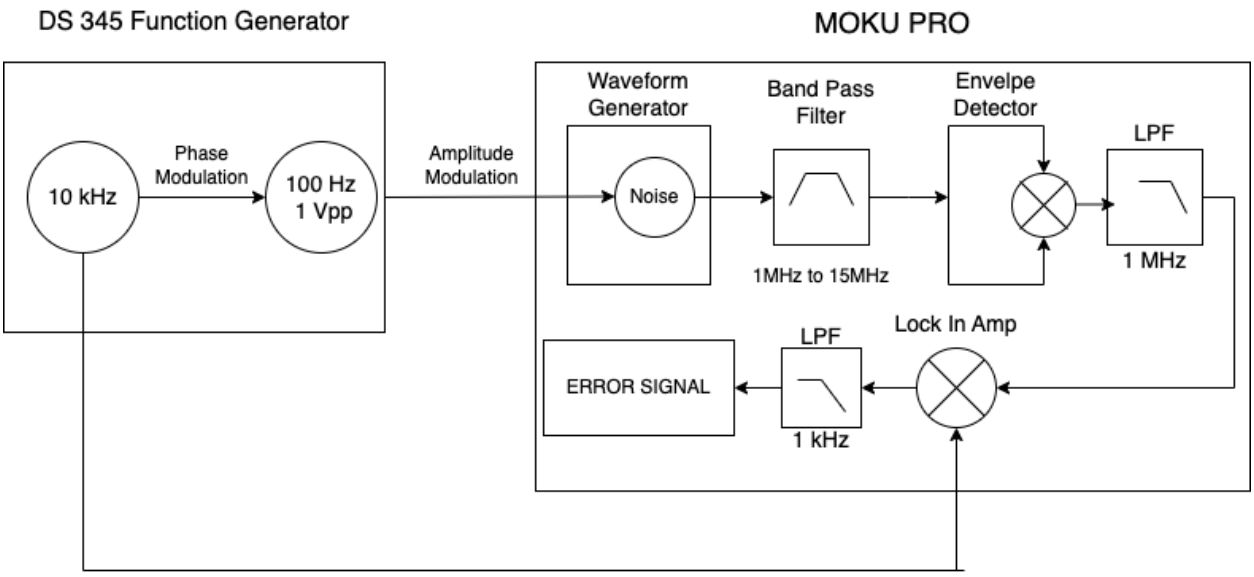

Figure 11: Schematic for the generation of error signal

the DS 345 function generator. The amplitude modulation would result in the rising and lowering of the noise amplitude, which corresponds to the effect of squeezing. The amplitude-modulated signal is sent into a Bandpass filter with the lower and upper cutoff as 1 MHz and 15 MHz, respectively. This is to make sure that we are obtaining the noise only in the bandwidth where the shot noise is present. The bandpass filtered output is the envelope detected (multiplied) that reads out the noise amplitude proportional to the actual input. This output is demodulated using the 10kHz dither signal in a lock-in amplifier and low pass filtered to produce the error signal.

The resulting error signal (in red) and the envelope detected output (in blue) are shown below in Figure 12.

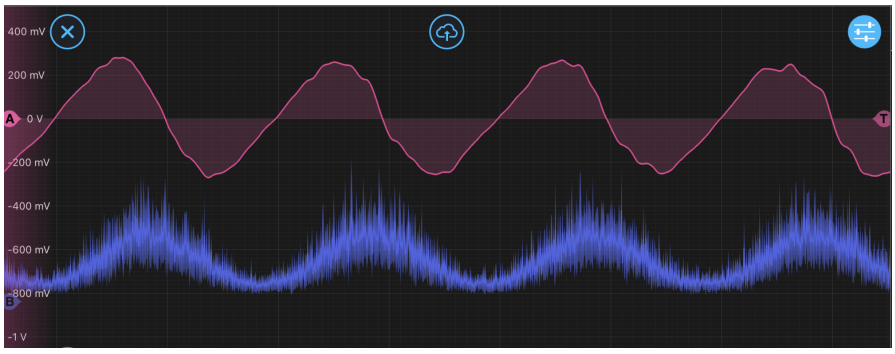

Figure 12: Error signal in Red and Envelope Detected Output in Blue

It can be noted that the error signal has zero crossings at those points where the noise amplitudes have their extrema. Noise amplitude or the envelope detected output having maxima correspond to the anti-squeezed quadrature and the minima to the squeezed quadrature. This shows that we can lock the squeeze angle to the squeezed or anti-squeezed curvature, as we have a 0V value for the error signal at those points. Thus, this matches the theoretical

predictions. It is also to be noted that the error signal appears distorted, which can be due to various low-pass filterings and multiplications. Once the performance of the technique is studied, the electronically simulated system is to be replaced by the optical squeezing setup, and the same noise-locking setup is to be implemented on this optical setup for obtaining phase locking.

5 Experiment

5.1 Control Loop Design

The control loop that we aim to produce for the optical setup is based on the following diagram:

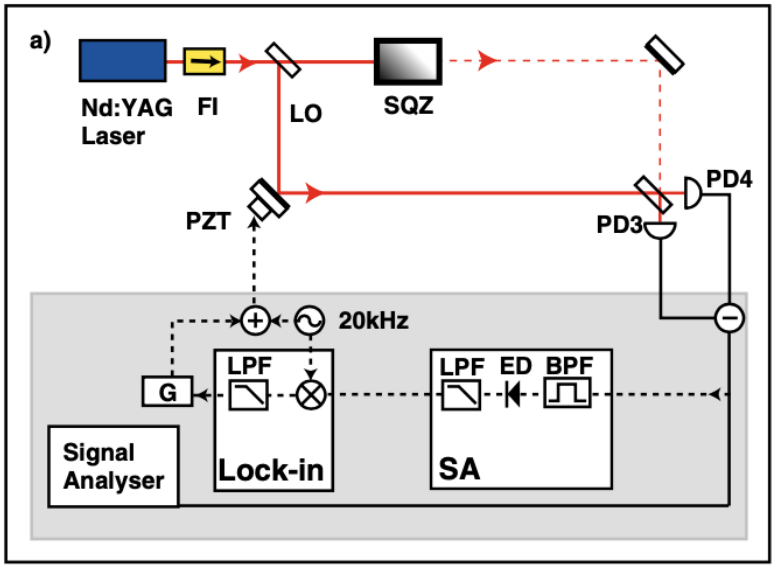

Figure 13: Schematic of the control loop for the optical system [6]

The objective was to work on the Noise locking part prior to working on the WOPA squeezing system. From the previous section, it was verified that MOKU could produce the desired error signal by reading off the variation in the noise amplitude. Thus, the further aim was to develop the electronic simulation of squeezing by taking into account the interferometric and seismic noises that can alter the homodyne angle and the balanced homodyne detection part. Once the electronic simulation of squeezing was done, the subsequent goal was to design the closed control loop and acquire the locking of the homodyne phase at minimum noise.

The control loop that was designed along with the electronic simulation for squeezing is shown below in Figure 13.

Here, the 1Hz signal (DC external signal in the case of 0V Amplitude) is summed with a 10kHz signal (simulates the motion of the PZT) to provide the signal for phase modulation. The low-frequency signal of 1Hz corresponds to the low-frequency seismic disturbances, which can affect the squeezing angle. This signal is passed on as phase modulation(3600°/V) to a 100kHz signal in the Moku Lab, which is further multiplied with another 100 kHz signal and low pass filtered (on low pass filter frequency cutoff is assigned such that only the DC component passes through after multiplication). The purpose of this is as follows: we need a 0Hz oscillator with phase modulation to obtain the lock and close the control loop in the electronic setup. So, this is a different way of obtaining the phase modulation information on a 0Hz signal. There is multiplication between two 100kHz sinusoidal signals, resulting in a signal with a DC part and a signal with twice the frequency, and we low pass filter the

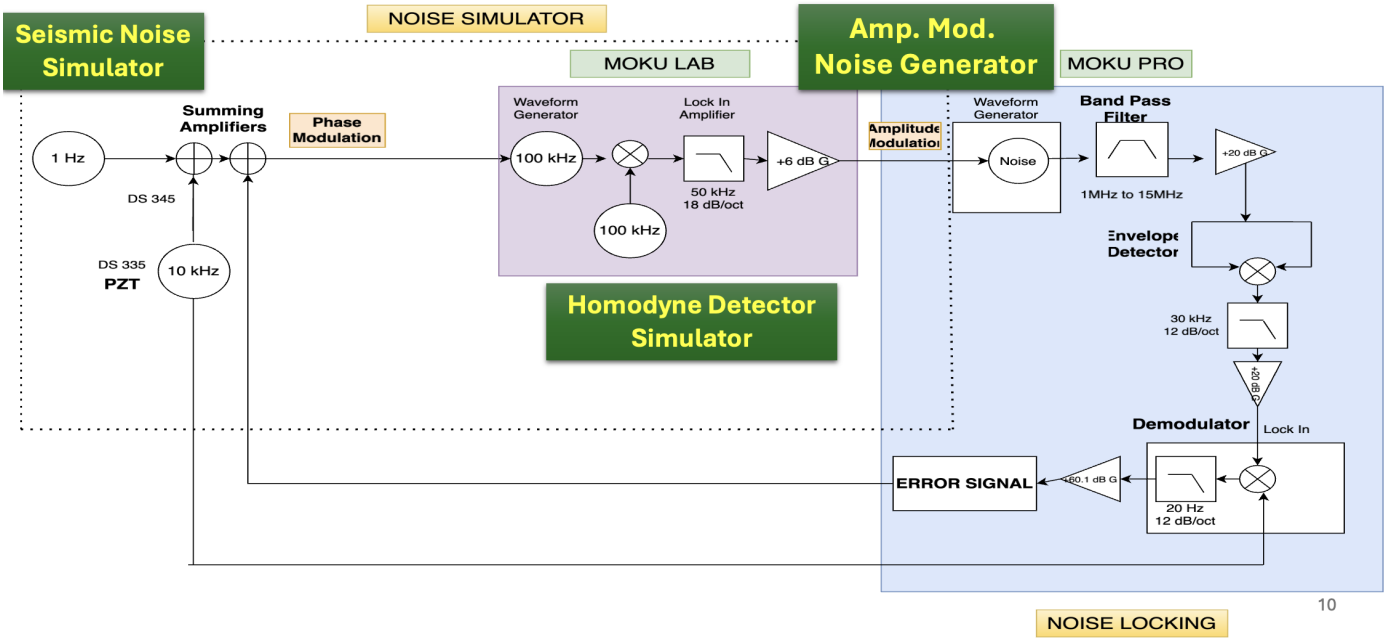

Figure 14: Schematic of the control loop

double frequency component. The resulting signal is passed onto the Moku Pro as the signal for Amplitude modulation, as described in the previous section. The Moku Pro functions as described previously to produce the error signal. As shown in the figure, the error signal was sent to another summing point and the summed signal was used for the further phase modulation.

Hence, this system electronically simulates the effect of squeezing with the help of amplitude modulation of generated noise, introduces seismic and interferometric disturbances that alter the homodyne phase, introduces dithering in the system as phase modulation, which corresponds to the function of PZT, performs Noise locking with MOKU PRO and produces the error signal which is further used as a feedback into the system. This is what the actual setup looks like:

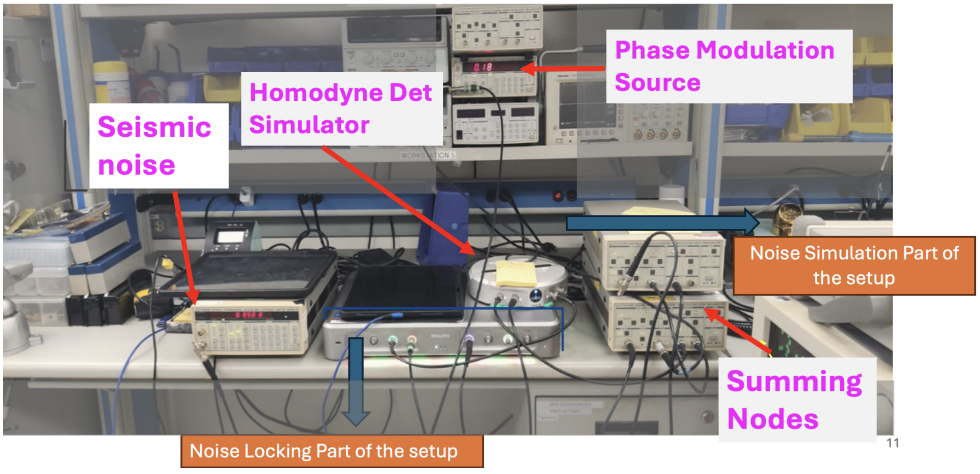

Figure 15: Control system

5.2 Acquiring the Lock

After tuning some of the parameters, including the gains in the lock-in amplifiers, the lock was achieved. The following diagram shows the varying noise amplitude before closing the loop. After the loop is closed (when the error signal is sent back into the simulated squeezing setup), it is seen that the noise amplitude acquires a constant value at the minimum of the noise level. This is shown below in Figure 15:

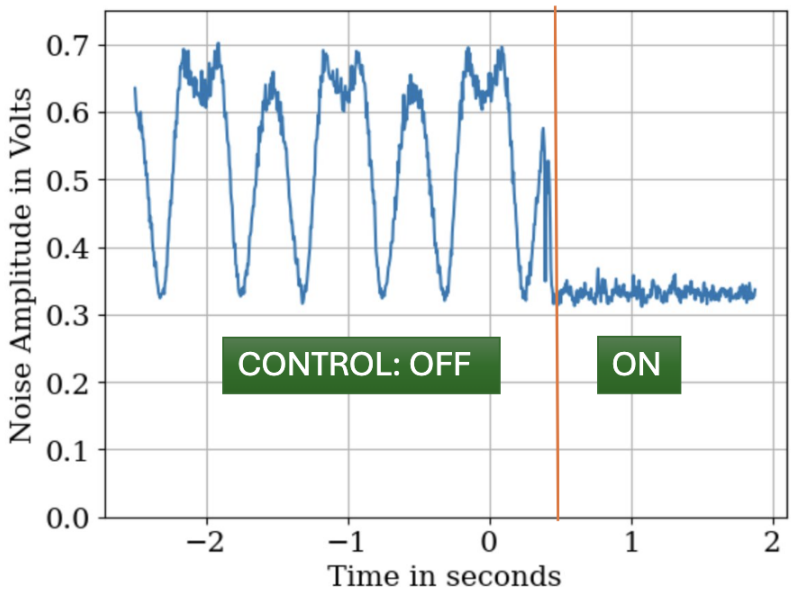

Figure 16: Envelope Detected output after locking onto the squeezed state

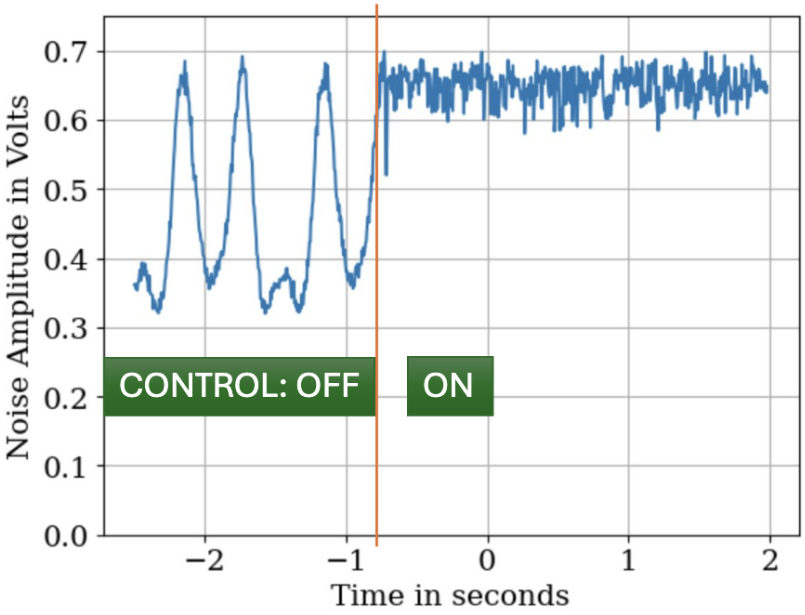

Figure 17: Envelope Detected output after locking onto the anti-squeezed state

It is to be noted that the error signal has zero crossings at the maximum noise amplitude level as well. Thus, it is also possible to lock on the anti-squeezed quadrature, as shown in the figure above. To lock it onto the anti-squeezed quadrature, the error signal was inverted by inverting the sign of one of the gains in the system. This resulted in the noise amplitude of the envelope-detected output achieving a maximum value, which shows that it is getting locked onto the anti-squeezed quadrature.

5.3 Orthogonality between the Error signal and the Envelope detected output

The static change of the homodyne angle can be achieved by giving 0 amplitude to the 1Hz disturbance signal and changing the DC offset value of that function generator. The corresponding value of change in phase can be calculated from the fact that we are providing the depth of the phase modulation as 3600 degrees per Volt (the maximum that Moku can do). On giving 0 amplitude to that signal, we measured the RMS Voltage of the constant error signal with varying values of the DC offset (a negative sign was given to RMS Voltage values when it went below zero). This is shown in Figure 11.

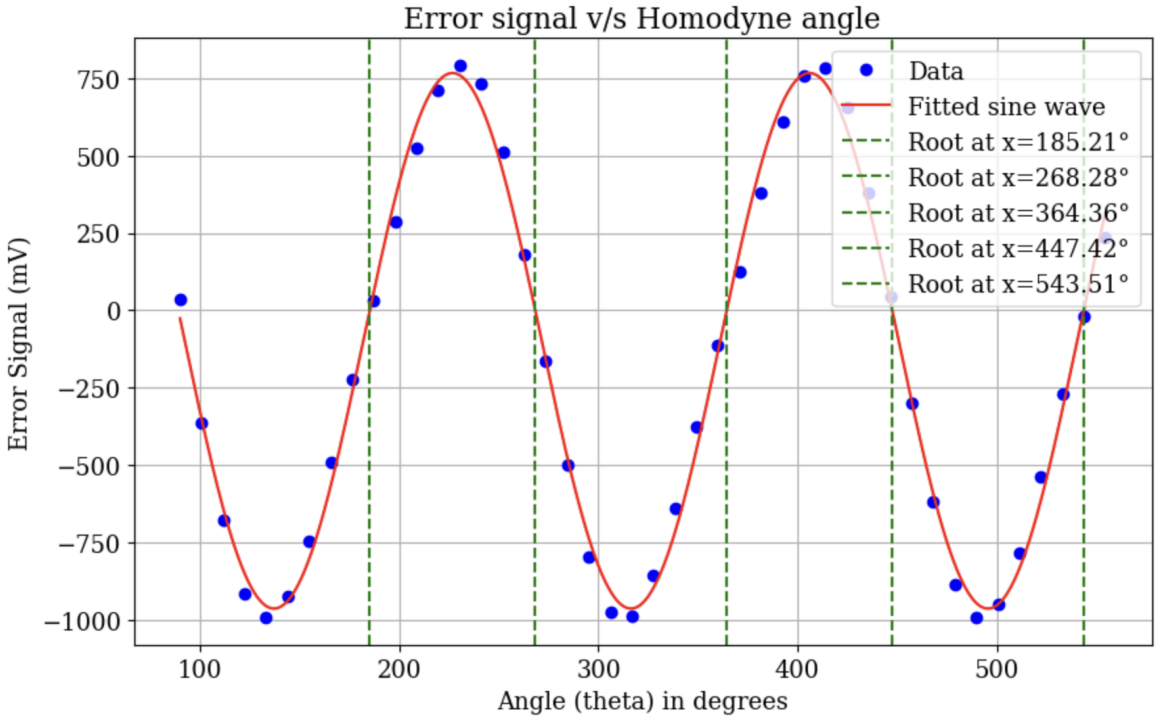

Figure 18: Error Signal after sinusoidal fit

The same was done for the envelope-detected output for the varying DC offset values. (This shows how the error signal and the noise amplitude vary with the phase). The data from the error signal was curve-fitted using a sinusoidal function, and the roots of the polynomial were found to correspond to the zero crossings of the error signal. The noise squared signal from the envelope detected output data was also plotted and sinusoidally fitted; the local minimum and maximum points were found, which correspond to the noise of the squeezed level and anti-squeezed level, respectively. This is shown in Figure 12.

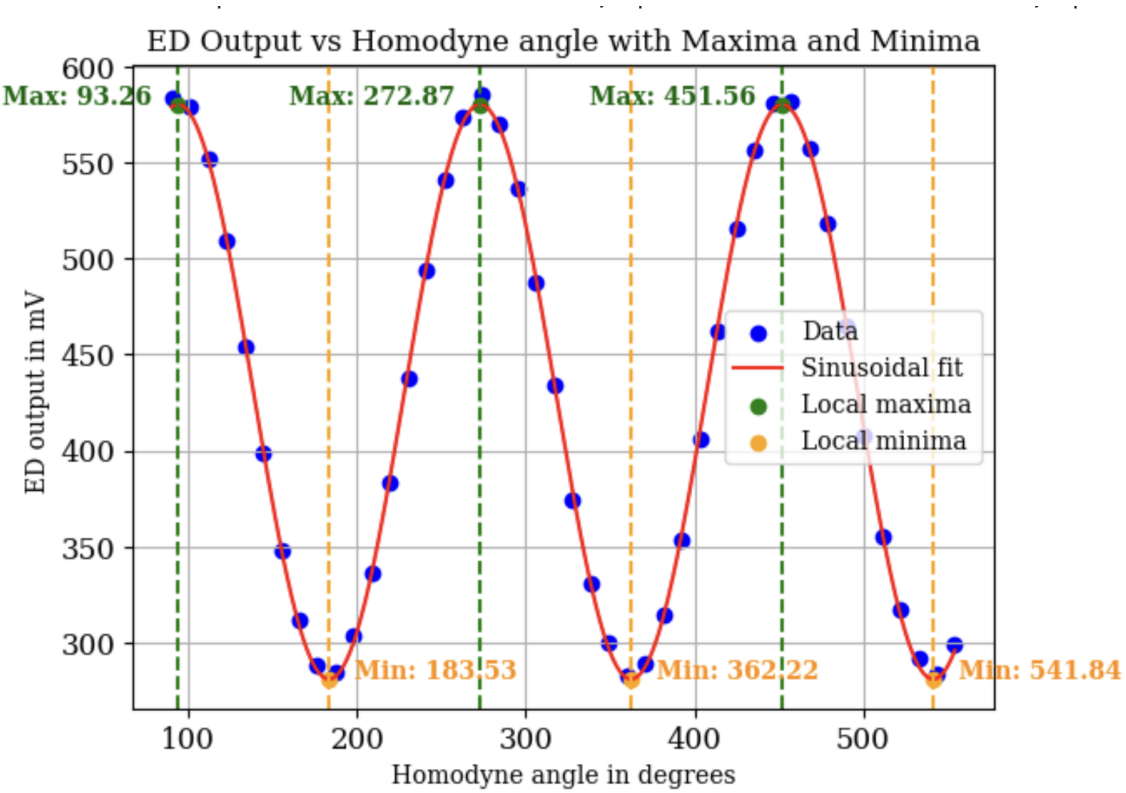

Figure 19: Envelope detected output after sinusoidal fit

The following table compares the zero crossings and the extrema (of the envelope detected output and the Bandpass filtered output). It is found that the average shift between these values is around 3-4° which shows that these two signals are orthogonal as was expected.

For sinusoidal fits

1)	**Zero Crossing of Error Signals (in °)**	277.14°	373.28°	456.14°	552.27°
2)	**Points of Extremum (ED output) (in °)**	281.28° (Max)	370.97° (Min)	460.66° (Max)	550.35° (Min)
3)	**Points of Extremum (BPF output) (in °)**	280.48° (Max)	370.97° (Min)	460.66° (Max)	550.35° (Min)
	Difference b/w 1 and 2 (in °)	4.14°	2.31°	4.52°	1.92°
	Difference b/w 1 and 3 (in °)	3.34°	2.31°	4.52°	1.92°

Figure 20: Table for comparing zero crossing and extrema phases

5.4 Measuring the Transfer function

The open loop transfer function of the system was measured for the loop characterisation using the spectrum analyser SRS785. Obtaining the open loop transfer function implies that the lock is stable, as it requires the stability of the lock for a period of time. The transfer function that was measured is shown in the Bode plot below:

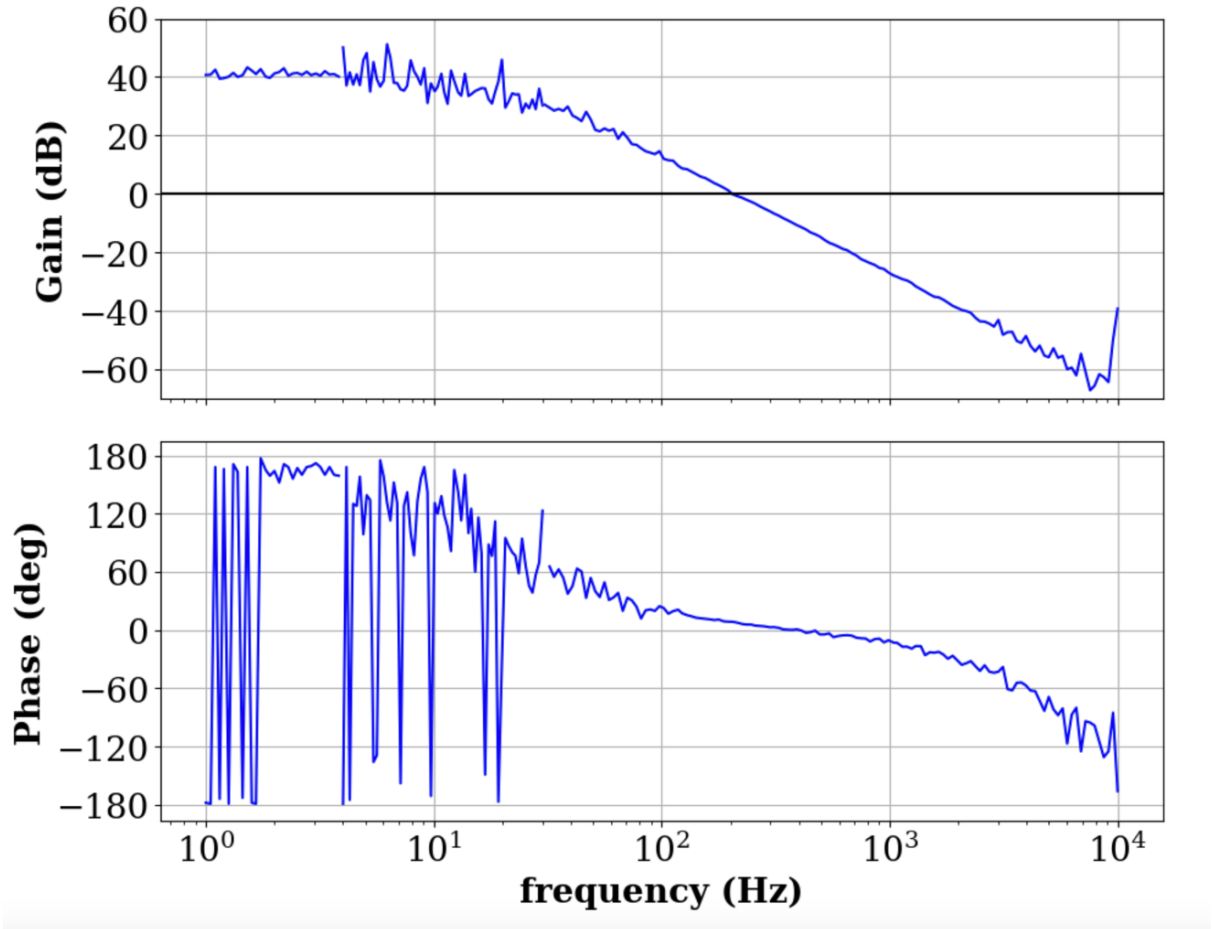

Figure 21: Open Loop Transfer Function for the control loop

From this, we obtained the unity gain frequency to be **200Hz**, which implies that the loop would be stable and the control will compensate for disturbances which have frequencies below 200Hz. Moreover, we have the suppression at DC to be 40dB, which implies that for disturbances close to 1Hz, it would get suppressed by a factor of **100**. It should also be noted that we need the phase margin to be at least 30-40 degrees at the unity gain frequency. But, from the transfer function bode plot, it could be seen that the phase margin is close to zero at the unity gain frequency. So, while working with the actual setup, we need a digital or an analog filter between the Moku PRO and the PZT to compensate for the phase margin at the unity gain frequency and also boost the gain below 20Hz so as to get more suppression of the external disturbances.

5.5 Sensor Noise Level

The noise injected by the sensor in the control was also determined. This was done by taking the spectrum of the noise of the error signal by fixing 0V amplitude for the 1Hz seismic disturbance. The amount of squeezing and anti-squeezing for this case was calculated to be -3.49 dB and +3 dB, respectively. The noise spectrum is as shown below:

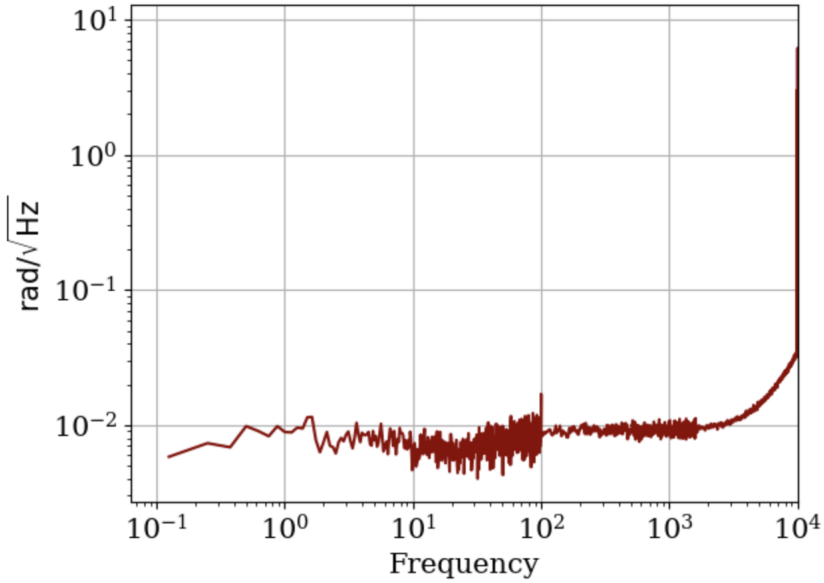

Figure 22: Sensor noise level

To obtain the calibrated noise level, we integrated the noise level up to the unity gain frequency and the injected noise level was found to be 0.1 rad.

5.6 Future Directions

The next step of the project is to use the noise locking onto the WOPA (Waveguide Optical Parametric Amplification) system and test its performance. The subsequent objective would be to mode-match the beam into the waveguide and obtain the squeezing arcs in the MHz frequency range and measure the squeezed quadrature using Balanced Homodyne Detection. The promising future direction would be to perform circuit noise analysis and readout optics/electronics to bring noise locking to the audio frequency regime, which would improve the sensitivity in the gravitational wave detection bandwidth. The proposed optical setup for WOPA is given below:

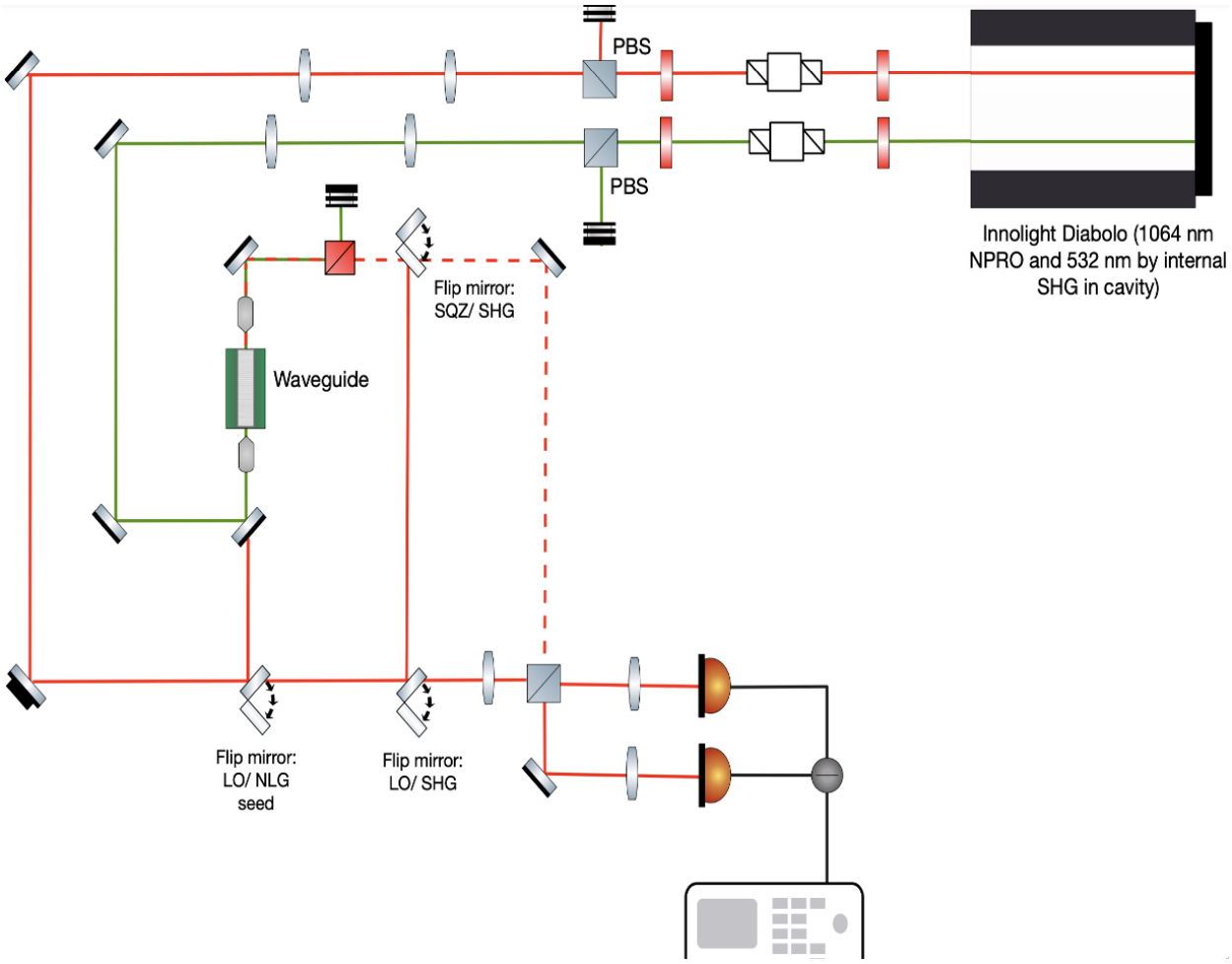

Figure 23: WOPA setup

6 Acknowledgements

I would like to thank LIGO, Caltech, Student-Faculty Programs and NSF for providing me with this opportunity to work on this project at West Bridge Labs. I want to extend my gratitude to mentors Dr. Koji Arai and Shruthi for their support. I would also like to thank Prof. Rana Adhikari for his constant guidance. I also want to thank Sarah Gates, another LIGO SURF student who worked with me on the project and the other SURFs for many interesting discussions.

References

[1] The LIGO Scientific Collaboration. *Advanced LIGO*. Classical and Quantum Gravity, 32, 7 (2015)

[2] G2401361, Koji Arai.*SURF Lecture GW Detector*

[3] Caves, Carlton M. *Quantum-mechanical noise in an interferometer* Phys. Rev. D, 23, 1693–1708.

[4] McKenzie, Kirk and Grosse, Nicolai and Bowen, Warwick P. and Whitcomb, Stanley E. and Gray, Malcolm B. and McClelland, David E. and Lam, Ping Koy *Squeezing in the Audio Gravitational-Wave Detection Band* Phys. Rev. Lett., 93, 161105, (2004)

[5] A. I. Lvovsky. *Squeezed light*. 2016.

[6] Kirk McKenzie and Eugeniy E Mikhailov and Keisuke Goda and Ping Koy Lam and Nicolai Grosse and Malcolm B Gray and Nergis Mavalvala and David E McClelland. *Quantum noise locking*. Journal of Optics B: Quantum and Semiclassical Optics, 7, 10.

7 Appendix

7.1 Noise Budget for the optical setup

The initial part of the project was to build the noise budget for the squeezing experiment. The following figures include the noise level in Amplitude Spectral Density (in $\frac{V}{\sqrt{Hz}}$) for the different sets of noise sources, including Moku base noise, Photodetector dark noise (in a lighted and dark room) and Laser noise.

All the measurements for the noise budget were made using the Spectrum Analyser instrument in the Moku, which has the option to give the noise level in the ASD (Amplitude Spectral Density) unit of $\frac{V}{\sqrt{Hz}}$.

Moku Noise floor: For the most part of this project, Moku instruments (Moku Pro, Moku Lab, Moku Go), a versatile set of high-performing measurement devices, would be used (especially for the noise locking part). Thus, the Moku noise floor for all the inputs that would be used was measured. This was done by switching ON various inputs of the Moku Spectrum Analyser and not connecting anything to it. This would give the noise floor of the Moku instrument itself.

Photodetector Dark Noise: The WOPA (Waveguide Optical Parametric Amplifier) squeezing setup uses Photo-receiver 1811 as the photodetector. Dark noise is an intrinsic source of noise present in photodetectors that arises from reasons like thermal agitation. This was measured by connecting the photodiode with the Moku and taking the spectrum of the noise that arises just from the surrounding light entering the photodetector. This measurement was done in a lighted room as well as in a dark room.

Laser RIN Noise: The Laser Noise was measured by inputting the laser used in the WOPA setup into the photodetector and then taking the spectrum. The power of the laser going into the photodetector was measured to be **0.5mW**.

Calculated level of shot noise: The estimated level of shot noise found in the plots below was determined based on Section 3.4 of this report.

All these above-mentioned noises are plotted in the noise budget plot below for two different frequency bandwidths. Figure 14 shows the noise level in the frequency range from 10Hz to 10kHz which and thus describes the level of noise in the audio bandwidth. Figure 15 shows the noise level in the noise level in the range from 10kHz to 1MHz. Figure 15 shows a compilation of these.

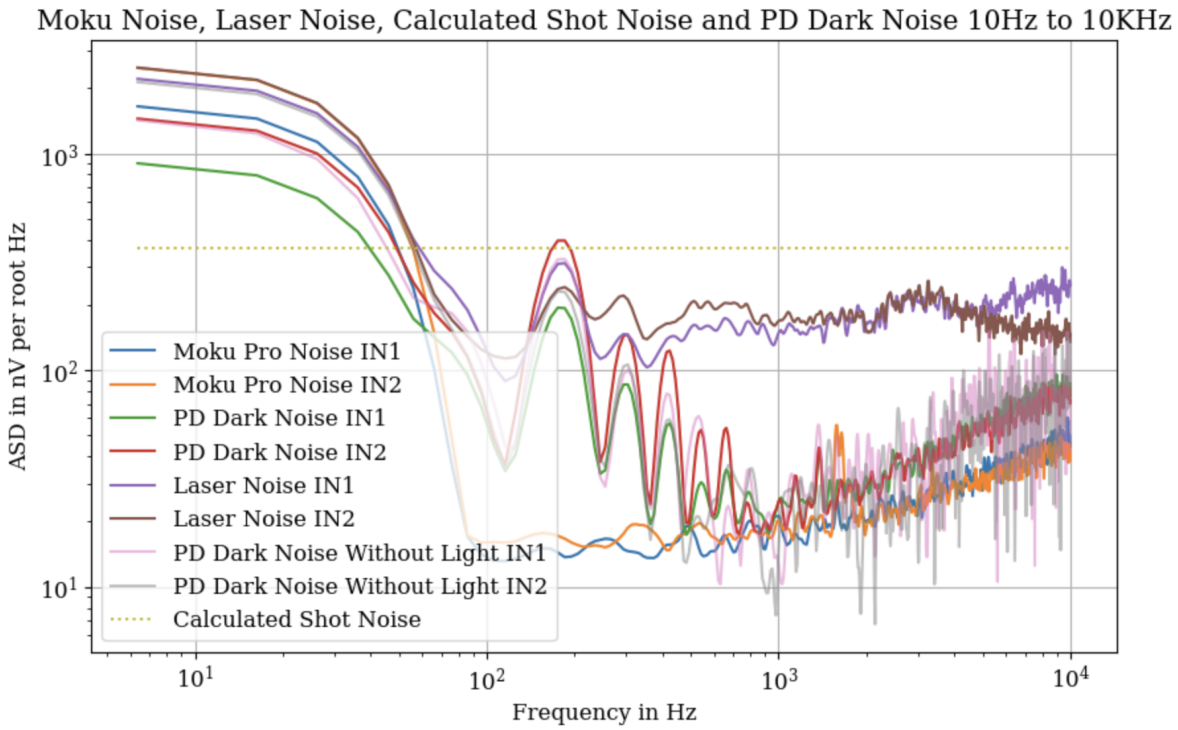

Figure 24: Noise Budget from 10Hz to 10KHz

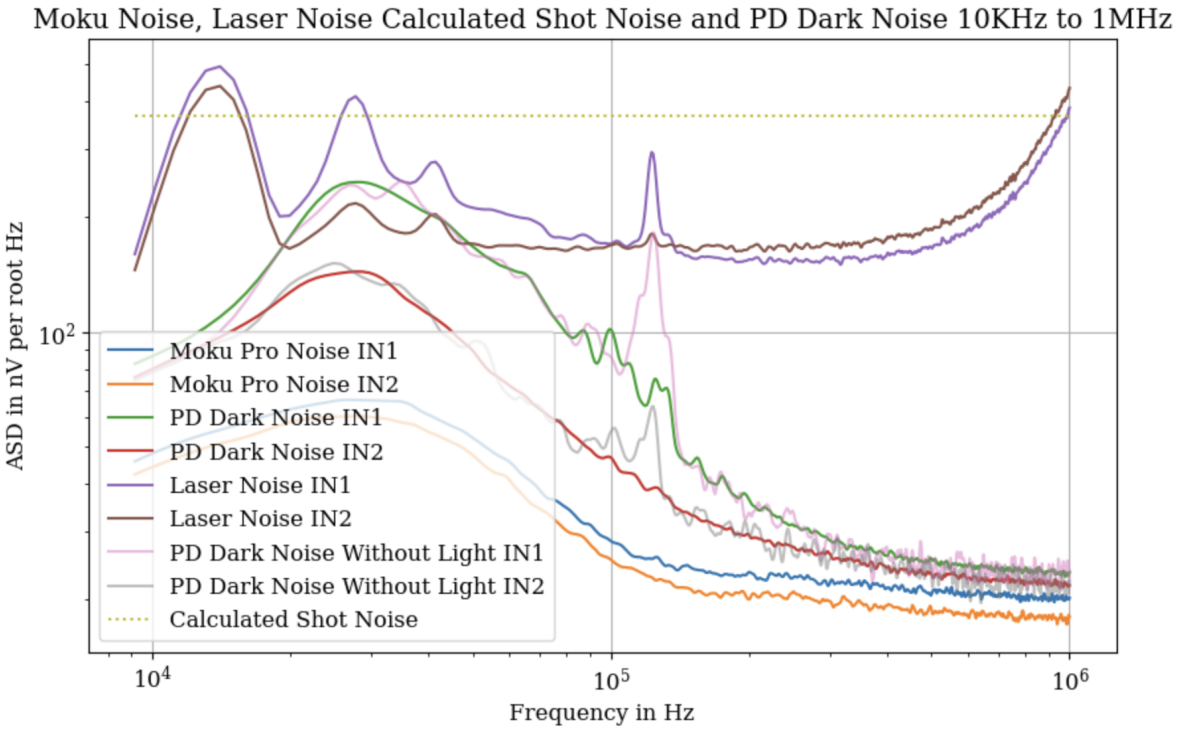

Figure 25: Noise budget from 10KHz to 1MHz

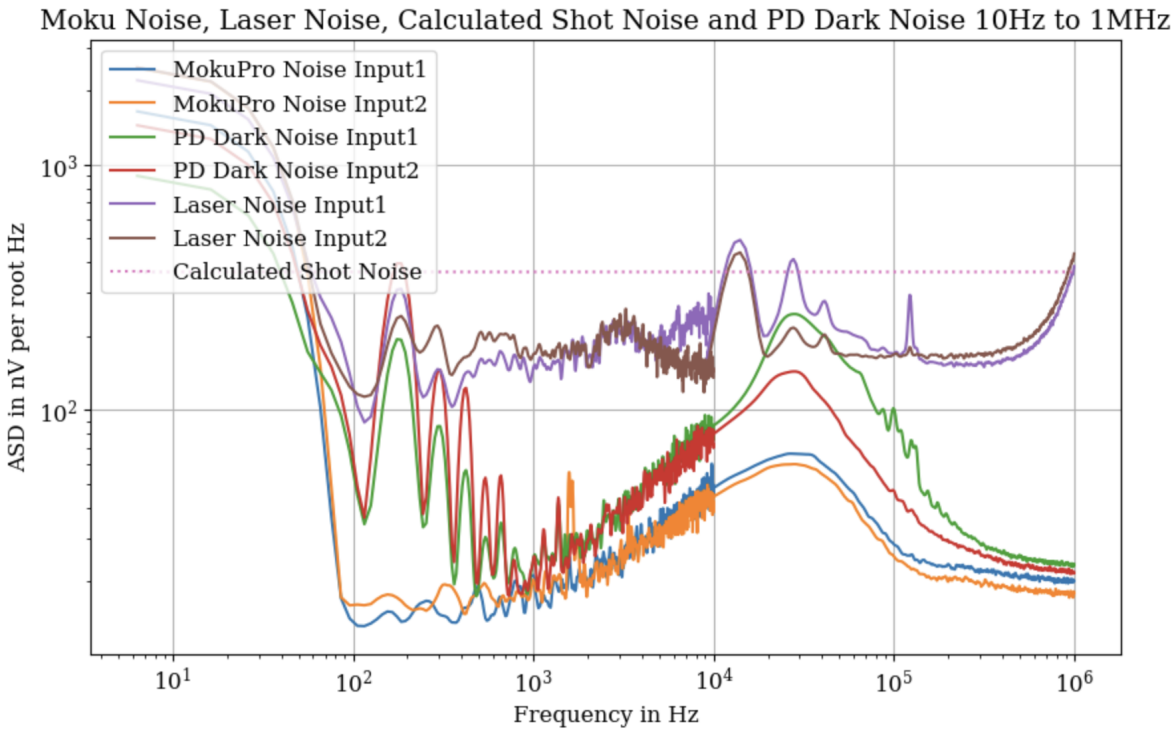

Figure 26: Noise budget from 10Hz to 1MHz

7.2 Calculating the level of squeezing and anti-squeezing the electronic simulation

The level of squeezing and anti-squeezing was calculated for the current electronic setup of Quantum Noise Locking. When there is 0% Amplitude modulation - it corresponds to the state where there is no squeezing, and thus, this simulates the level of shot noise (in the electronic setup, it is simulated by the noise generator of the Moku). This level was measured as the Voltage RMS in the envelope detected output in the Moku Pro, and this turned out to be 4.298 mV (V_{shot}).

Then, a 100% per Volt Amplitude Modulation was imposed onto the Moku-generated noise. The signal used for this modulation is the same as in the recent setup. The change in the homodyne angle is simulated by changing the DC offset level of the 1Hz disturbance signal at 0 Volt amplitude. This allows us to measure the maximum and minimum levels of the envelope detected output as the DC offset is varied. The minimum voltage RMS was measured to be 3.650 mV ($V_{squeezed}$); this corresponds to the squeezed noise level. The maximum voltage RMS was measured to be 5.001 mV ($V_antisqueezed$), which corresponds to the anti-squeezed level.

The level of squeezing in dB was measured using the formula:

$$\text{Squeezing in dB} = 20log(V_{squeezed}/V_{shot})$$

$$\text{Anti Squeezing in dB} = 20log(V_{antisqueezed}/V_{shot})$$

Using this, the level of squeezing was found to be -1.41 dB. The level of anti-squeezing is 1.315 dB.

The same calculation was done for 250% per Volt amplitude modulation. This resulted in -3.8 dB squeezing and 3.14 dB anti-squeezing.

Note: The difference in the level of squeezing and anti-squeezing can be accounted for by the distortion that is seen in the error signal as well.